SYNTHESIS

CHAPTER 1

Fluorinated Peroxides as Initiators of Fluorinated Polymers

SHOHEI YAMAZAKI* AND HIDEO SAWADA

Department of Frontier Materials Chemistry, Graduate School of Science and Technology, Hirosaki University, Hirosaki 036-8561, Japan
*Email: shy@hirosaki-u.ac.jp

1.1 Introduction

It is in general well known that alkanoyl peroxides [R–C(=O)–O–O–(O=)C–R; R = alkyl group] decompose homolytically *via* a stepwise radical fission to produce an acyloxy radical [R–C(=O)O$^{\bullet}$] and finally an alkyl radical (R$^{\bullet}$), as shown in Scheme 1.1.[1] However, interestingly, fluoroalkanoyl peroxides [R_F–C(=O)–O–O–(O=)C–R_F; R_F = fluoroalkyl group] can decompose homolytically through three-bond radical fission to afford fluoroalkyl radicals ($R_F^{\bullet}$; see Scheme 1.2).[1] This unique decomposition mechanism has already been applied as a radical initiator for fluoroolefins such as tetrafluoroethylene to produce thermally stable fluorinated polymers.[2,3] The thermal stability of the fluorinated polymers thus obtained is due to the direct introduction of fluoroalkyl segments (R_F) related to the peroxide into the fluorinated polymer end-chains (R_F–$CF_2CF_2\sim$) during the radical polymerization process of fluoroolefins initiated by fluoroalkanoyl peroxides.[1–3] The thermal decomposition of fluoroalkanoyl peroxides selectively affords the corresponding coupling products (R_F–R_F) in good yields, indicating the formation of $R_F^{\bullet}$ radicals during the decomposition process (see Scheme 1.2), although

RSC Polymer Chemistry Series No. 23
Fluorinated Polymers: Volume 1: Synthesis, Properties, Processing and Simulation
Edited by Bruno Ameduri and Hideo Sawada

Published by the Royal Society of Chemistry, www.rsc.org

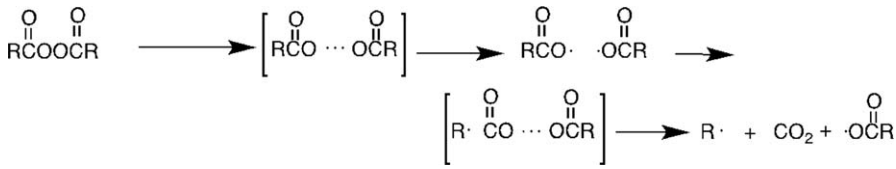

Scheme 1.1 Thermal decomposition of alkanoyl peroxides.

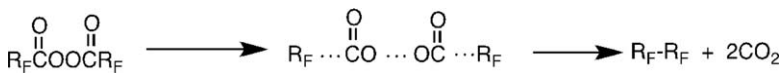

Scheme 1.2 Thermal decomposition of fluoroalkanoyl peroxides.

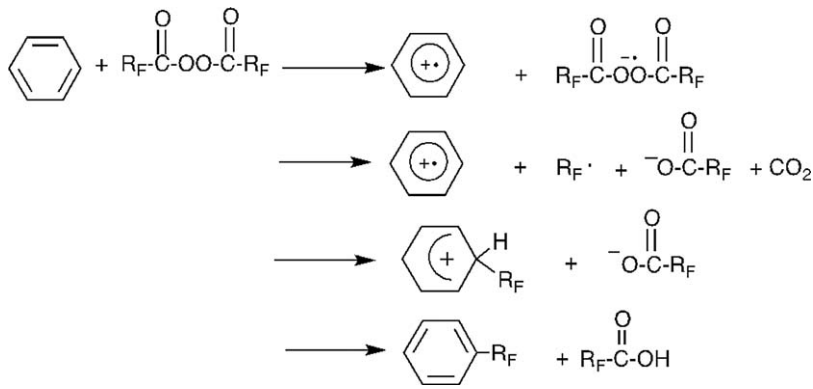

Scheme 1.3 Direct introduction of a fluoroalkyl group (R_F) into benzene through the single electron transfer reaction from benzene to fluoroalkanoyl peroxide.

the corresponding non-fluorinated alkanoyl peroxide affords the ester products [R–C(=O)OR] through stepwise radical decomposition fission (see Scheme 1.1).[1]

Another specific characteristic of fluoroalkanoyl peroxides is that they are useful electron acceptors even from well-known relatively poor electron-donor aromatic compounds such as benzene, chlorobenzene and hetero-aromatic compounds such as thiophenes and furan to proceed *via* a single electron transfer reaction from these aromatic compounds to the peroxide.[4,5] As shown in Scheme 1.3, this single electron transfer reaction permits the direct introduction of a fluoroalkyl group (R_F) related to the peroxide into the corresponding aromatic compounds in good yields.[4,5] In this way, fluoroalkanoyl peroxides can exhibit considerably different properties from those of the corresponding non-fluorinated compounds.

It is of great interest how fluorination improves the reactivity of alkanoyl peroxides so substantially. For the understanding of the effects of fluorination, it is useful to elucidate the electronic structures of alkanoyl and fluoroalkanoyl peroxides, because the alkyl and fluoroalkyl groups exhibit

significantly different electronic properties, especially a much higher electronegativity of the fluorine atom than the hydrogen atom. In this chapter, the electronic structure of alkanoyl/fluoroalkanoyl peroxides is studied computationally using *ab initio* molecular orbital methods. In 1990, Sawada *et al.*[6] performed a computational study of these peroxides using a semiempirical molecular orbital method, in which some parameters were determined from experimental data. *Ab initio* methods, on the other hand, use no empirical parameters in the calculation of molecular electronic structure. The advantage of *ab initio* over semiempirical methods is that one can systematically improve the accuracy of the molecular wavefunction, in principle, towards the exact solution of Schrödinger equation. An *ab initio* method involves a much larger computational cost than a semiempirical method. Owing to recent progress in computer technology, however, today it is not difficult to carry out *ab initio* calculations on alkanoyl/fluoroalkanoyl peroxides when the size of the alkyl/fluoroalkyl group is relatively small.

In the case of the introduction of fluoroalkyl groups into aromatic compounds (Scheme 1.3), previous computational studies revealed how fluorination significantly improves the reactivity.[1,6] According to molecular orbital calculations, the LUMO (lowest unoccupied molecular orbital) of a fluoroalkanoyl peroxide exhibits considerably lower energy than that of the corresponding non-fluorinated alkanoyl peroxide. This stabilization significantly reduces the energy difference from the HOMO (highest occupied molecular orbital) of aromatic compounds. As a result, the HOMO–LUMO interaction of fluoroalkanoyl peroxides is much larger than that of non-fluorinated alkanoyl peroxides, which leads to a higher efficiency of electron transfer from aromatic compounds to fluoroalkanoyl peroxides.

With respect to thermal decomposition (Schemes 1.1 and 1.2), some computational studies with *ab initio* methods have been performed for the dissociation of alkanoyl/fluoroalkanoyl peroxides and acyloxy radicals.[7–9] However, it is unclear why fluoroalkanoyl and alkanoyl peroxides exhibit quite different decomposition mechanisms.

In the present work, we performed computational studies of the thermal decomposition of alkanoyl/fluoroalkanoyl peroxides. Our goal was to clarify the effect of fluorination on the mechanism of decomposition at the molecular level. In particular, our aim was to elucidate what determines whether the decomposition occurs *via* a stepwise or a concerted mechanism. As the first step in achieving this goal, this chapter focuses on the properties of O–O and C–C bonds and the energetics of thermal decomposition.

1.2 Computational Methods

Ab initio electronic structure calculations were performed for alkanoyl/fluoroalkanoyl peroxides [RC(O)O–OC(O)R] (hereafter R denotes both alkyl and fluoroalkyl groups and the double bond in the chemical formula is omitted) and their fragments including RC(O)O$^{\bullet}$ and R$^{\bullet}$ radicals. Electronic energies of these compounds were calculated with the second-order

Møller–Plesset (MP2) method, a perturbation method for evaluating electron correlation energies using the Hartree–Fock wavefunction as reference. The restricted Hartree–Fock (RHF) and restricted open-shell Hartree–Fock (ROHF) methods were applied for the calculation of the reference wavefunction of closed-shell systems (peroxides, *etc.*) and open-shell systems (radicals), respectively. The Sapporo-DZP-2012 basis set, recently developed by Noro *et al.*,[10] was employed for all calculations (DZP is the abbreviation for double zeta with polarization), hereafter denoted DZP. The molecular structure in the electronic ground state was optimized at the MP2/DZP level, where symmetry of the C_2 point group was assumed for RC(O)O–OC(O)R peroxides and no symmetry constraint was imposed for other compounds. Normal-mode analysis was also performed for the optimized structures, in order to confirm that they are minimum-energy structures with no imaginary-frequency mode and to estimate the zero point energy (ZPE) of each compound. All calculations were carried out using the GAMESS program package.[11]

1.3 Results and Discussion

For alkanoyl/fluoroalkanoyl peroxides [RC(O)O–OC(O)R], it was proposed that non-fluorinated alkanoyl peroxides decompose in a stepwise manner, whereas fluoroalkanoyl peroxides decompose in a concerted manner, as discussed in the Introduction.[1] In the case of alkanoyl peroxides, the decomposition is likely to occur in two steps (see also Scheme 1.1). In the first step, the RC(O)O–OC(O)R peroxide undergoes homolytic dissociation of the central O–O bond to produce an RC(O)O$^\bullet$ radical:

$$\mathrm{RC(O)O\text{–}OC(O)R} \rightarrow 2\mathrm{RC(O)O}^\bullet \tag{1.1}$$

In the second step, the RC(O)O$^\bullet$ radical decomposes to the R$^\bullet$ radical and a CO_2 molecule by dissociation of the C–C bond:

$$\mathrm{RC(O)O}^\bullet \rightarrow \mathrm{R}^\bullet + \mathrm{CO_2} \tag{1.2}$$

The intermediate RC(O)O$^\bullet$ leads to the formation of ester products (see the Introduction), which are thermally less stable. In the case of fluoroalkanoyl peroxides, on the other hand, the decomposition into an R$^\bullet$ radical and a CO_2 molecule occurs in a single step, that is, by concerted dissociation of the O–O bond and two C–C bonds of RC(O)O–OC(O)R (see also Scheme 1.2):

$$\mathrm{RC(O)O\text{–}OC(O)R} \rightarrow 2\mathrm{R}^\bullet + 2\mathrm{CO_2} \tag{1.3}$$

Direct formation of the R$^\bullet$ radical results in the selective production of thermally stable fluorinated polymers that do not have an ester group.

Another interesting observation in the thermal decomposition of alkanoyl/fluoroalkanoyl peroxides is that the decomposition rate depends strongly on the substituent R.[6] In particular, the rate of decomposition of fluoroalkanoyl peroxides is much higher than that of non-fluorinated alkanoyl peroxides.

In this section, we computationally examine the molecular structure of RC(O)O–OC(O)R peroxides (Section 1.3.1), the molecular structure of RC(O)O• radicals produced by homolytic dissociation according to eqn (1.1) (Section 1.3.2), the bond dissociation energy (BDE) of peroxides and radicals (Section 1.3.3) and the heat of reaction for thermal decomposition according to eqn (1.3) (Section 1.3.4), focusing on the peroxides that have a methyl/fluoromethyl group or ethyl/fluoroethyl group as R. To elucidate the effects of fluorination on molecular properties in more detail, we studied partially fluorinated compounds in addition to non-fluorinated and perfluorinated compounds.

1.3.1 Molecular Structure of Alkanoyl/Fluoroalkanoyl Peroxides

Figure 1.1 shows the equilibrium geometry of RC(O)O–OC(O)R peroxides whose R substituent is a methyl or fluoromethyl group (R = CH_3, CH_2F, CHF_2 and CF_3), optimized with the MP2/DZP method. The length of the central O1–O1′ bond (see Figure 1.1a for the atom labeling of peroxides) is around 1.45 Å for all compounds, a typical value for the O–O single bond of peroxides. The C2–O1–O1′–C2′ group is largely twisted, with dihedral angles of 77.5, 79.1, 80.4 and 80.3° for R = CH_3, CH_2F, CHF_2 and CF_3, respectively. These dihedral angles are much smaller than the H–O–O–H dihedral angle

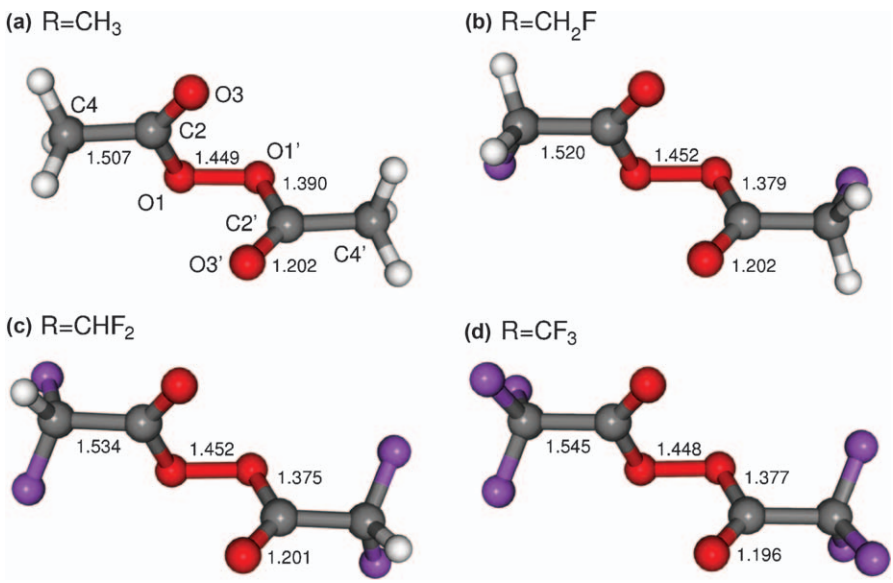

Figure 1.1 Molecular structure of RC(O)O–OC(O)R peroxides for (a) R = CH_3, (b) R = CH_2F, (c) R = CHF_2 and (d) R = CF_3, optimized at the MP2/DZP level of theory. Bond lengths in Å. Panel (a) also shows the atom labeling for O and C.

of hydrogen peroxide, calculated to be 115.0° by geometry optimization at the MP2/DZP level. The small dihedral angle of the C–O–O–C group is supported by previous theoretical and experimental studies,[8,12] and is also found in peroxides with other electron-withdrawing groups, *e.g.* FO–OF and ClO–OCl.[13]

The optimized structures in Figure 1.1 indicate that the C2–C4 bond, *i.e.* the C–C bond adjacent to the central O–O group and assumed to dissociate by thermal decomposition of peroxide, becomes substantially longer with fluorination of the R group, whereas the O–O and O–C bond lengths are very similar for all compounds. The C2–C4 bond distances optimized at the MP2/DZP level are 1.507, 1.520, 1.534 and 1.545 Å for R = CH_3, CH_2F, CHF_2 and CF_3, respectively. The C2′–C4′ bond of each peroxide exhibits the same length as the C2–C4 bond due to the C_2 symmetry of the molecular structure. The present results suggest that the introduction of F atoms on the R group substantially weakens the bond between the R group and the adjacent C atom.

As shown in Figure 1.1, the length of C2–O3 and C2′–O3′ bonds is 1.20 Å for all four compounds, reflecting the formation of a C–O double bond. On the other hand, the C2–O1 and C2′–O1′ bonds exhibit a distance of about 1.4 Å, which indicates that they form a single bond.

The CC(O)O part of each RC(O)O moiety exhibits a nearly planar structure, that is, O1, C2, O3 and C4 atoms (or O1′, C2′, O3′ and C4′ atoms) are located almost in the same plane. Each of the C2–O3 and C2′–O3′ bonds is syn-periplanar to the O1–O1′ bond, that is, O1′, O1, C2 and O3 atoms are located almost in the same plane, and this also applies for O1, O1′, C2′ and O3′ atoms.

Geometry optimization at the MP2/DZP level was also performed for RC(O)O–OC(O)R peroxides with R being an ethyl or fluoroethyl group. Table 1.1 gives the O1–O1′ and C2–C4 (or C2′–C4′) bond lengths and the C2–O1–O1–C2′ dihedral angles of peroxides when R is an ethyl/fluoroethyl group and also a methyl/fluoromethyl group. For comparison, Table 1.1 also gives the O–O bond lengths and C–O–O–C dihedral angles of HC(O)O–OC(O)H (R = H) and the O–O bond length and H–O–O–H dihedral angle of hydrogen peroxide, where the molecular structures of HC(O)O–OC(O)H and hydrogen peroxide were optimized with the MP2/DZP method.

As can be seen in Table 1.1, the O1–O1′ bond distance seems to be nearly independent of the number of F atoms in the R substituent in the case of an ethyl/fluoroethyl group, as in the case of a methyl/fluoromethyl group. The length of the O1–O1′ bond is around 1.45 Å for all ethyl and fluoroethyl groups and the lengths differ in the order of 0.001 Å from one another (the same applies for methyl/fluoromethyl groups; see also Figure 1.1). HC(O)O–OC(O)H and hydrogen peroxide exhibit slightly larger lengths of the O–O bond, 1.454 and 1.460 Å, respectively, but the difference from those of alkanoyl/fluoroalkanoyl peroxides is still very small.

On the other hand, the C2–C4 (and C2′–C4′) bond distance of peroxides with R being an ethyl/fluoroethyl group exhibits a clear dependence on the

Table 1.1 Selected geometric parameters [O1–O1′ bond distances r(O1–O1′), C2–C4 bond distances r(C2–C4) and C2-O1–O1′–C2′ dihedral angles δ(C2–O1–O1′–C2′)] of RC(O)O–OC(O)R peroxides determined with MP2/DZP geometry optimization, and bond orders (BOs) of O1–O1′ and C2–C4 calculated with the RHF/DZP method for the optimized geometry.

R	r(O1–O1′)/Å	BO(O1–O1′)	r(C2–C4)/Å[a]	BO(C2–C4)[a]	δ(C2–O1–O1′–C2′)/°
CH_3	1.449	0.931	1.507	1.069	77.5
CH_2F	1.452	0.934	1.520	1.036	79.1
CHF_2	1.452	0.934	1.534	0.998	80.4
CF_3	1.448	0.938	1.545	0.990	80.3
CH_2–CH_3	1.452	0.932	1.512	1.043	77.0
CH_2–CH_2F	1.453	0.932	1.514	1.026	76.8
CH_2–CHF_2	1.452	0.933	1.510	1.024	76.7
CH_2–CF_3	1.450	0.935	1.514	1.007	79.1
CHF–CH_3	1.449	0.935	1.522	0.998	74.7
CHF–CH_2F	1.449	0.936	1.521	0.986	73.9
CHF–CHF_2	1.448	0.941	1.521	0.999	77.0
CHF–CF_3	1.448	0.938	1.528	0.986	74.6
CF_2–CH_3	1.451	0.939	1.539	0.984	75.3
CF_2–CH_2F	1.453	0.939	1.540	0.961	79.3
CF_2–CHF_2	1.450	0.940	1.542	0.971	77.3
CF_2–CF_3	1.449	0.941	1.542	0.974	76.0
H	1.454	0.808			80.9
Hydrogen peroxide	1.460	0.879			115.0[b]

[a]C2–C4 is the C–C bond adjacent to the O–O group (see Figure 1.1a for atom labeling).
[b]H–O–O–H dihedral angle, *i.e.* δ(H–O–O–H).

number of F atoms in the methylene bridge at the C4 position (CH_2, CHF or CF_2). The length of the C2–C4 bond determined at the MP2/DZP level is 1.510–1.514 Å for the CH_2 bridge, 1.521–1.528 Å for the CHF bridge and 1.539–1.542 Å for the CF_2 bridge (see Table 1.1). For the R group with the same methylene/fluoromethylene bridge, the bond length is likely to be almost independent of the number of F atoms in the terminal methyl/fluoromethyl group (CH_3, CH_2F, CHF_2 or CF_3). The C2–C4 bond lengths differ by less than 0.01 Å among CH_3, CH_2F, CHF_2 and CF_3. In addition, no significant correlation is found between the bond length and the number of F atoms in the terminal group.

Table 1.1 also shows bond order of O1–O1′ and C2–C4 for alkanoyl/fluoroalkanoyl peroxides, calculated at the RHF/DZP level at the MP2-optimized geometry. As expected from the bond distance, the bond order of O1–O1′ exhibits very similar values for all compounds, whereas the bond order of C2–C4 depends significantly on the number of F atoms. In the case of methyl/fluoromethyl groups, the O1–O1′ bond order is 0.931, 0.934, 0.934 and 0.938 and the C2–C4 bond order is 1.069, 1.036, 0.998 and 0.990 for R = CH_3, CH_2F, CHF_2 and CF_3, respectively. The latter result suggests that the C2–C4 bond is weakened by fluorination of the methyl group. In the case of ethyl/fluoroethyl groups, the C2–C4 bond order is largely reduced by fluorination of the methylene bridge at the C4 position. Fluorination of the

terminal methyl group is also likely to reduce the bond order, but the extent of the reduction is smaller than for the methylene bridge. For example, the C2–C4 bond order is 1.043 for $R = CH_2CH_3$, but 0.984 and 1.007 for $R = CF_2CH_3$ and CH_2CF_3, respectively.

As in the case of methyl/fluoromethyl groups, the C2–O1–O1′–C2′ part exhibits a dihedral angle of about 80° in the case of ethyl/fluoroethyl groups (see Table 1.1). This dihedral angle is less likely to correlate with the number of F atoms. It should be noted that HC(O)O–OC(O)H also exhibits a very similar dihedral angle, whereas hydrogen peroxide exhibits a much larger dihedral angle of H–O–O–H, as mentioned above. The C–O–O–C dihedral angle of HC(O)O–OC(O)H and the H–O–O–H dihedral angle of hydrogen peroxide are 80.9° and 115.0°, respectively. This finding suggests that the small C–O–O–C dihedral angle of alkanoyl/fluoroalkanoyl peroxides can be attributed to the carbonyl group (C2–O3 group), which is largely electron withdrawing.

The CC(O)O part of peroxides with ethyl/fluoroethyl groups exhibits similar features to those with methyl/fluoromethyl groups. The lengths of the C2–O3 and C2–O1 bonds are about 1.2 and 1.4 Å, respectively. Each CC(O)O part is in a nearly planar structure and the C2–O3 bond is synperiplanar to the O1–O1′ bond.

1.3.2 Molecular Structure of Alkanoyl/Fluoroalkanoyl Radicals

Figure 1.2 shows the MP2-optimized equilibrium geometry of $RC(O)O^{\bullet}$ radicals, produced by homolytic dissociation of RC(O)O–OC(O)R peroxides [eqn (1.1)] with R being a methyl or fluoromethyl group. As in the case of the parent peroxides, the C2–C4 bond length becomes larger as the number of F atoms in the methyl group increases (see Figure 1.2a for the atom labeling of radicals). The bond distance is 1.514, 1.524, 1.538 and 1.548 Å for $R = CH_3$, CH_2F, CHF_2 and CF_3, respectively. This result suggests that weakening of the C–C bond by fluorination occurs in $RC(O)O^{\bullet}$ radicals as well as in RC(O)O–OC(O)R peroxides.

Table 1.2 summarizes the C2–C4 bond lengths of $RC(O)O^{\bullet}$ radicals with R being a methyl/fluoromethyl or ethyl/fluoroethyl group. For the latter, the C2–C4 bond distance becomes longer with fluorination of the methylene bridge: the bond length is 1.519–1.522 Å for the CH_2 group, 1.528–1.540 Å for the CHF group and 1.543–1.548 Å for the CF_2 group. Within each methylene/fluoromethylene bridge, the bond length exhibits very similar values for all terminal methyl/fluoromethyl groups.

The bond order of C2–C4, calculated at the ROHF/DZP level, is also summarized in Table 1.2. It is clearly shown that the C2–C4 bond order of $RC(O)O^{\bullet}$ radicals decreases with fluorination of the R group as in the case of RC(O)O–OC(O)R peroxides, especially with fluorination of the methyl group or methylene bridge adjacent to the C2 atom. For example, the C2–C4 bond

order is 1.044, 1.011, 0.974 and 0.963 for R = CH_3, CH_2F, CHF_2 and CF_3, respectively. These values are slightly smaller than the corresponding bond orders of RC(O)O–OC(O)R peroxides, suggesting that the C–C bond becomes weaker due to homolytic dissociation.

For each RC(O)O• radical with R being a methyl/fluoromethyl group, the two C–O bonds differ in length from each other by more than 0.1 Å (see Figure 1.2). The C2–O1 bond afforded by dissociation of the C–O–O–C group of the parent peroxide exhibits the length of about 1.34 Å for all compounds. On the other hand, the C2–O3 bond exhibits a length of about 1.21 Å, close to the C2–O3 bond length in the parent RC(O)O–OC(O)R peroxide. The same applies for RC(O)O• radicals with ethyl/fluoroethyl groups. These results strongly suggest that the radicals retain the R–C2(=O3)–O1• resonance structure, that is, the C2–O1 and C2–O3 bonds remain single and double bonds, respectively, and the unpaired electron is localized on the O1 atom. As in the case of RC(O)O–OC(O)R peroxide, the CC(O)O part of the RC(O)O• radical exhibits a nearly planar structure.

It should be noted that the molecular structure of the RC(O)O• radical potentially has the problem of symmetry breaking.[7] In other words, the unpaired electron might be delocalized over the symmetrical OCO framework rather than localized on one of the two oxygen atoms.[7] However, the

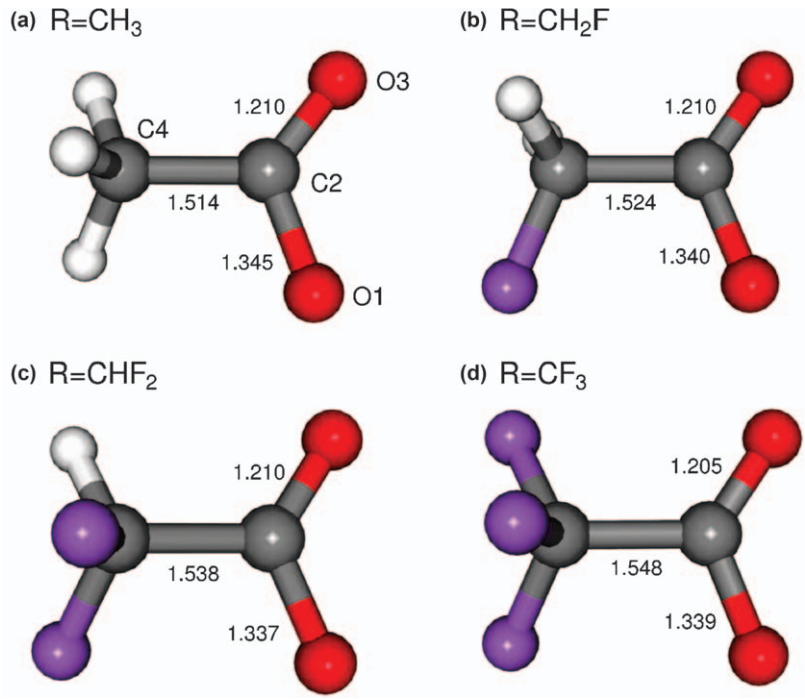

Figure 1.2 Molecular structure of RC(O)O• radicals for (a) R = CH_3, (b) R = CH_2F, (c) R = CHF_2 and (d) R = CF_3, optimized at the MP2/DZP level of theory. Bond lengths in Å. Panel (a) also shows the atom labeling for O and C.

Table 1.2 Bond distances of C2–C4 of RC(O)O• radicals determined with MP2/DZP geometry optimization and bond orders (BOs) of C2–C4 calculated with the ROHF/DZP method for the optimized geometry.

R	r(C2–C4)/Å	BO(C2–C4)
CH_3	1.514	1.044
CH_2F	1.524	1.011
CHF_2	1.538	0.974
CF_3	1.548	0.963
CH_2–CH_3	1.520	1.023
CH_2–CH_2F	1.522	1.000
CH_2–CHF_2	1.519	1.001
CH_2–CF_3	1.522	0.999
CHF–CH_3	1.533	0.973
CHF–CH_2F	1.533	0.961
CHF–CHF_2	1.528	0.970
CHF–CF_3	1.540	0.965
CF_2–CH_3	1.545	0.952
CF_2–CH_2F	1.543	0.942
CF_2–CHF_2	1.548	0.938
CF_2–CF_3	1.546	0.941

MP2 method, a single-reference perturbation method for the calculation of electron correlation, is not adequate for treating symmetric and asymmetric structures, where the unpaired electron is delocalized and localized, respectively, on an equal footing. This is because the reference Hartree–Fock wavefunction is represented by a superposition of two resonance structures in the symmetric geometry, R–C2(=O3)–O1• and R–C2(=O1)–O3•, but by only one resonance structure in the asymmetric geometry. This qualitative difference in reference wavefunction leads to an artificial difference in MP2-calculated electron correlation energies. A multi-reference electron-correlation method such as MRCI (multi-reference configuration interaction) would be necessary to avoid this problem. In the present work, we focused on the asymmetric geometry discussed above. The main scope of the present work – the effect of fluorination on the reactivity of alkanoyl peroxides – is expected to be little affected by the difference in symmetry of the OCO part, because this symmetry would influence the electronic structure of all compounds in a similar way.

1.3.3 Bond Dissociation Energy of Alkanoyl/Fluoroalkanoyl Peroxides and Radicals

On the basis of the molecular structures discussed in Sections 1.3.1 and 1.3.2, one can expect that the strength of the O–O bond of RC(O)O–OC(O)R peroxides is little affected by fluorination, whereas the C–C bond assumed to dissociate in thermal decomposition is significantly weakened by fluorination of the methyl group or methylene bridge adjacent to the OCO part in

the case of both RC(O)O–OC(O)R peroxides and RC(O)O$^{\bullet}$ radicals. In this section, we discuss the BDE of the O–O and C–C bonds to clarify the character of these bonds in more detail.

The O–O BDE of peroxides (BDE of the O1–O1′ bond) is calculated as the change in electronic energy by the homolytic dissociation reaction (1.1), the first step of the stepwise decomposition:

$$\mathrm{BDE(O\text{–}O,\ peroxide)} = 2E[\mathrm{RC(O)O^{\bullet}}] - E[\mathrm{RC(O)O\text{–}OC(O)R}] \qquad (1.4)$$

where E[RC(O)O–OC(O)R] and E[RC(O)O$^{\bullet}$] are the electronic energies of the RC(O)O–OC(O)R peroxide and RC(O)O$^{\bullet}$ radical, respectively, calculated with the MP2/DZP method. The geometry of each compound is optimized at the same computational level.

The C–C BDE of peroxide (BDE of the C2–C4 or C2′–C4′ bond) is calculated by the following equation:

$$\mathrm{BDE(C\text{–}C,\ peroxide)} = E_{\mathrm{frozen}}[\mathrm{RC(O)O\text{–}OCO^{\bullet}}] + E_{\mathrm{frozen}}(\mathrm{R^{\bullet}}) - E[\mathrm{RC(O)O\text{–}OC(O)R}] \qquad (1.5)$$

where E_{frozen}[RC(O)O–OCO$^{\bullet}$] and E_{frozen}(R$^{\bullet}$) are the MP2/DZP electronic energies of RC(O)O–OCO$^{\bullet}$ and R$^{\bullet}$ radicals, respectively. The subscript ''frozen'' indicates that the geometries of RC(O)O–OCO$^{\bullet}$ and R$^{\bullet}$ radicals are frozen to that in the parent RC(O)O–OC(O)R peroxide for the calculation of electronic energies. Although we tried geometry optimization of the fragments, the RC(O)O–OCO$^{\bullet}$ radical was decomposed to an RC(O)O$^{\bullet}$ radical and a CO_2 molecule.

The O–O and C–C BDEs of RC(O)O–OC(O)R peroxides are summarized in Table 1.3. For the O–O BDE, the results of ZPE correction are also included in the table, where the ZPEs of reactant (peroxide) and product (radical) calculated at the MP2/DZP level were added to E[RC(O)O–OC(O)R] and E[RC(O)O$^{\bullet}$], respectively.

For the O–O bond, the BDEs of all compounds exhibit similar values. In the case of a methyl/fluoromethyl group, the O–O BDE is calculated as 234.1, 228.9, 230.2 and 231.0 kJ mol^{-1} for R = CH_3, CH_2F, CHF_2 and CF_3, respectively, without ZPE correction. The corresponding BDE with ZPE correction is 219.0, 215.0, 216.5 and 218.2 kJ mol^{-1}. In the case of an ethyl/fluoroethyl group, the minimum BDE value is 227.6 kJ mol^{-1} without ZPE correction (214.7 kJ mol^{-1} with ZPE correction) for R = CF_2–CH_2F, while the maximum value is 251.3 kJ mol^{-1} without ZPE correction (237.2 kJ mol^{-1} with ZPE correction) for R = CHF–CH_2F. Because of these results, one can conclude that fluorination of the R group is hardly likely to affect the strength of the O–O bond of alkanoyl peroxides, as expected from the bond length and bond order discussed in Section 1.3.1. This finding also implies that the substituent dependence of the mechanism and kinetics of thermal decomposition could not be attributed to effects of fluorination on the character of the O–O bond.

Table 1.3 Bond dissociation energies (BDEs) for O1–O1′ and C2–C4 bonds of RC(O)O–OC(O)R peroxides, labeled BDE(O–O, peroxide) and BDE(C–C, peroxide), respectively, and BDE for the C2–C4 bond of RC(O)O• radicals, labeled BDE(C–C, radical) (in kJ mol^{-1}).

R	BDE(O–O, peroxide)[a]	BDE(C–C, peroxide)[b]	BDE(C–C, radical)[a]
CH_3	234.1 (219.0)	457.7	−106.9 (−124.8)
CH_2F	228.9 (215.0)	423.9	−127.4 (−140.8)
CHF_2	230.2 (216.5)	396.2	−143.3 (−151.6)
CF_3	231.0 (218.2)	396.5	−139.8 (−145.0)
CH_2–CH_3	234.4 (220.3)	457.7	−106.3 (−122.1)
CH_2–CH_2F	235.5 (221.7)	459.8	−104.4 (−120.0)
CH_2–CHF_2	236.7 (223.2)	461.7	−105.0 (−118.8)
CH_2–CF_3	237.9 (224.2)	454.1	−114.0 (−127.6)
CHF–CH_3	248.0 (233.8)	431.1	−132.5 (−143.0)
CHF–CH_2F	251.3 (237.2)	434.3	−136.2 (−145.9)
CHF–CHF_2	241.9 (228.2)	431.6	−132.6 (−142.2)
CHF–CF_3	239.5 (226.4)	423.4	−136.7 (−146.1)
CF_2–CH_3	232.9 (220.0)	408.9	−136.5 (−142.7)
CF_2–CH_2F	227.6 (214.7)	407.3	−132.0 (−138.0)
CF_2–CHF_2	233.3 (220.3)	405.4	−138.1 (−143.3)
CF_2–CF_3	234.4 (221.6)	403.4	−142.1 (−147.1)

[a]Values in parentheses are corrected with zero point energy.
[b]Geometry of each fragment is frozen to that in the parent peroxide.

The BDE of the C–C bond of peroxides, on the other hand, exhibits a large dependence on the substituent. For methyl/fluoromethyl group, the C–C BDE decreases as the number of F atoms increases. The calculated values are 457.7, 423.9, 396.2 and 396.5 kJ mol^{-1} for R = CH_3, CH_2F, CHF_2 and CF_3, respectively. The BDEs for R = CHF_2 and R = CF_3 are very similar in spite of the fact that the latter exhibits a longer C–C bond and a higher bond order (see also Table 1.2). This may be because, in these peroxides, the electron repulsion interactions between the fluoromethyl group and the OCO part differ from each other. For the ethyl/fluoroethyl group, fluorination of the methylene bridge substantially reduces the C–C BDE. The calculated values are 454.1–461.7 kJ mol^{-1} for the CH_2 bridge, 423.4–434.3 kJ mol^{-1} for the CHF bridge and 403.4–408.9 kJ mol^{-1} for the CF_2 bridge. Within the same methylene/fluoromethylene bridge, the BDE is little affected by fluorination of the terminal methyl/fluoromethyl group. The computational results for the C–C BDE for the methyl/fluoromethyl and ethyl/fluoroethyl groups clearly indicate that the C2–C4 bond is substantially weakened by the fluorination on the C4 atom rather than that on other C atoms such as the terminal C atom of the ethyl/fluoroethyl group. The weakening of the C2–C4 bond may be attributed to withdrawal of the electron on the C4 atom by the F atom, which may lead to the reduction of bond order shown in Table 1.1 and electrostatic repulsion between the fluoromethyl or fluoroethyl group and the OCO part in each RC(O)O• moiety. Since the C2–C4 bond dissociates in thermal decomposition of RC(O)O–OC(O)R peroxides, it is expected that the decrease in BDE on fluorination would be responsible for the different

reaction mechanisms and different reaction rates between alkanoyl and fluoroalkanoyl peroxides.

We also calculated the C–C BDE (BDE of the C2–C4 bond) of $RC(O)O^{\bullet}$ radicals. The C–C BDE of radicals is calculated as the change in electronic energy by the reaction in eqn (1.3), the second step of the stepwise decomposition:

$$\mathrm{BDE(C\text{–}C,\ radical)} = E(R^{\bullet}) + E(CO_2) - E[RC(O)O^{\bullet}] \qquad (1.6)$$

where $E(R^{\bullet})$ and $E(CO_2)$ are the electronic energies of the $R^{\bullet}$ radical and CO_2 molecule, respectively, calculated with the MP2/DZP method. The geometry of each compound is optimized at the same computational level. As a result of geometry optimization, $E(R^{\bullet})$ in eqn (1.6) is about 10–30 kJ mol^{-1} lower than $E_{\mathrm{frozen}}(R^{\bullet})$ in eqn (1.5) for each R group. In the case of $R = CH_3$, for example, the MP2-calculated values of $E(R^{\bullet})$ and $E_{\mathrm{frozen}}(R^{\bullet})$ are $-39.6926E_h$ and $-39.6824E_h$, respectively, which differ by 26.7 kJ mol^{-1} (E_h is the atomic unit of energy; $1E_h = 2625.5$ kJ mol^{-1}).

The calculated C–C BDEs of $RC(O)O^{\bullet}$ radicals are given in Table 1.3, where the ZPE-corrected BDEs are also shown. The computational results suggest that the C2–C4 bond is weakened by the fluorination of the methyl group or methylene bridge adjacent to the OCO part, as in the case of RC(O)O–OC(O)R peroxides. For a methyl/fluoromethyl group, the C–C BDE is -106.9, -127.4, -143.3 and -139.8 kJ mol^{-1} without ZPE correction (-124.8, -140.8, -151.6 and -145.0 kJ mol^{-1} with ZPE correction) for $R = CH_3$, CH_2F, CHF_2 and CF_3, respectively. For an ethyl/fluoroethyl group, the BDE is considerably decreased by fluorination of the methylene bridge. The calculated values without ZPE correction (with ZPE correction) are from -114.0 to -104.4 kJ mol^{-1} (from -127.6 to -118.8 kJ mol^{-1}) for the CH_2 bridge, from -136.7 to -132.5 kJ mol^{-1} (from -146.1 to -142.2 kJ mol^{-1}) for the CHF bridge and from -142.1 to -132.0 kJ mol^{-1} (from -147.1 to -138.0 kJ mol^{-1}) for the CF_2 bridge.

As shown in Table 1.3, the C–C BDEs of $RC(O)O^{\bullet}$ radicals are much lower than those of RC(O)O–OC(O)R peroxides. Therefore, one can expect that the C–C bond of radicals is much weaker than that of peroxides. It is necessary to keep in mind, however, that the geometry of the fragments is optimized for the calculation of the C–C BDE of radicals, but not for that of peroxides; see eqn (1.5) and (1.6). This difference in computational procedure indicates that the difference between the BDEs of peroxides and radicals may be largely overestimated. In the case of CH_3, for example, the C–C BDE of the $RC(O)O^{\bullet}$ radical is calculated to be 236.8 kJ mol^{-1} at the MP2/DZP level when the geometries of fragments $R^{\bullet}$ and CO_2 are frozen. In particular, the CO_2 molecule is substantially bent when the geometry is frozen, which results in a much higher energy (by more than 300 kJ mol^{-1}) than the energy in the optimized linear geometry.

Figure 1.3 shows a schematic plot of the potential energy curve for the C–C bond dissociation of the $RC(O)O^{\bullet}$ radical [eqn (1.3)] expected from the present computational results. For $R = CH_3$, Zhou *et al.*[9] calculated a

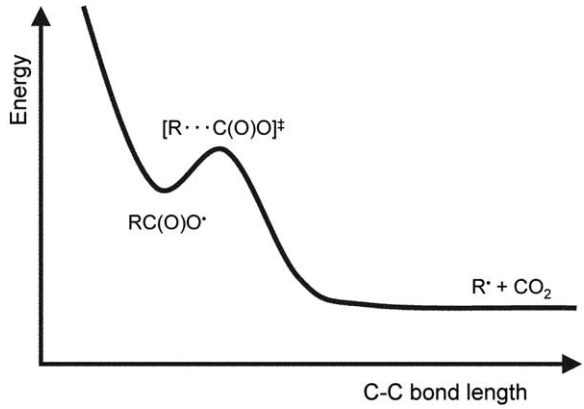

Figure 1.3 Schematic representation of the potential energy curve for the dissociation reaction $RC(O)O^{\bullet} \rightarrow R^{\bullet} + CO_2$.

potential energy curve very similar to that in Figure 1.3. The potential energy curve in Figure 1.3 exhibits several important features. First, since the C–C BDE of the $RC(O)O^{\bullet}$ radical is calculated to be negative (see Table 1.3), the product of dissociation, *i.e.* the molecular system including the $R^{\bullet}$ radical and CO_2 molecule, is energetically more stable than the reactant, *i.e.* the $RC(O)O^{\bullet}$ radical. Second, since the equilibrium geometry of the $RC(O)O^{\bullet}$ radical is located (see Figure 1.2), the potential energy curve exhibits a minimum corresponding to this radical. Finally, and more importantly, because of the first and second features, there should exist a barrier for the C–C dissociation and transition state structure corresponding to the barrier, denoted $[R\cdots C(O)O]^{\ddagger}$ in Figure 1.3. Zhou *et al.*[9] and Gu *et al.*[8] located the transition state structure with the MP2 method for $R = CH_3$ and for $R = CH_3$ and CF_3, respectively.

The barrier of the C–C dissociation originates from transformation of the singly occupied molecular orbital (SOMO) of the $RC(O)O^{\bullet}$ radical. Figure 1.4 shows the SOMO of $RC(O)O^{\bullet}$ and $R^{\bullet}$ radicals for $R = CH_3$ and CF_3, calculated at the ROHF/DZP level for each optimized structure. The SOMO of the $RC(O)O^{\bullet}$ radical is the non-bonding p orbital on the O1 atom (see Figure 1.2 for atom labeling), whereas the SOMO of the $R^{\bullet}$ radical is mainly contributed from the p orbital on the C4 atom. The same applies for other R groups. Note that the SOMO of the $RC(O)O^{\bullet}$ radical is localized on one of the two O atoms. This result supports the R–C(=O)–$O^{\bullet}$ resonance structure of the radical, as expected from the molecular structure (see Section 1.3.2). As shown in Figure 1.4a, the $CH_3^{\bullet}$ radical exhibits a planar structure and the SOMO of this radical is likely to correspond to a pure p orbital on the C atom. On the other hand, the $CF_3^{\bullet}$ radical shows a pyramidal structure and the SOMO exhibits a small mixing of p orbitals on the F atoms with the p orbital on the C atom (see Figure 1.4b).

1.3.4 Thermal Decomposition of Alkanoyl/Fluoroalkanoyl Peroxides

The heat of reaction for the concerted thermal decomposition of RC(O)O–OC(O)R peroxide [eqn (1.3)], denoted ΔE, is calculated as follows:

$$\Delta E = 2E(\mathrm{R}^{\bullet}) + 2E(\mathrm{CO_2}) - E[\mathrm{RC(O)O{-}OC(O)R}] \tag{1.7}$$

The geometry of the fragments $\mathrm{R}^{\bullet}$ and $\mathrm{CO_2}$ and also that of RC(O)O–OC(O)R peroxide are optimized at the MP2/DZP level. From eqn (1.4) and (1.6), the heat of decomposition ΔE in eqn (1.7) can be rewritten using the O–O BDE of RC(O)O–OC(O)R peroxide and the C–C BDE of $\mathrm{RC(O)O}^{\bullet}$ radical:

$$\Delta E = \mathrm{BDE(O{-}O,\ peroxide)} + 2\mathrm{BDE(C{-}C,\ radical)} \tag{1.8}$$

Table 1.4 summarizes the heat of decomposition ΔE of RC(O)O–OC(O)R peroxides with R being a methyl/fluoromethyl or ethyl/fluoroethyl group, calculated using eqn (1.7) or (1.8). The ΔE values are lowered considerably by fluorination of the methyl group or methylene bridge. Therefore, the thermal decomposition is likely to be more exothermic for fluoroalkanoyl peroxides than for non-fluorinated alkanoyl peroxides. Because of eqn (1.8), the lower heat of decomposition can be attributed to the lower BDE of the C–C bond.

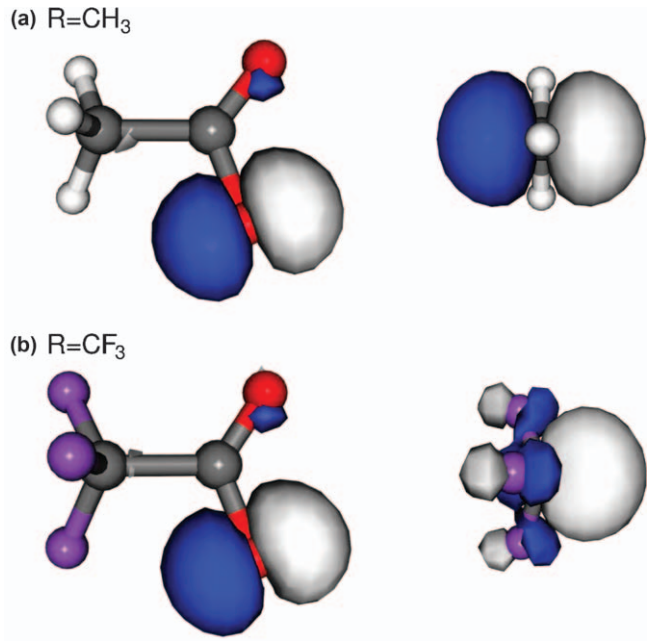

Figure 1.4 SOMO of $\mathrm{RC(O)O}^{\bullet}$ radicals (left) and $\mathrm{R}^{\bullet}$ radicals (right) for (a) $\mathrm{R = CH_3}$ and (b) $\mathrm{R = CF_3}$, calculated at the ROHF/DZP level of theory.

Table 1.4 Computational heats of decomposition ΔE and experimental rates of decomposition k_d of RC(O)O–OC(O)R peroxides.

R	ΔE/kJ mol^{-1}[a]	$k_d/s^{-1}\times10^8$
CH_3	20.3 (−30.7)	2[b,c]
CH_2F	−25.9 (−66.5)	
CHF_2	−56.4 (−86.6)	
CF_3	−48.7 (−71.9)	100[b,d]
CH_2–CH_3	21.7 (−23.9)	3[b,c]
CH_2–CH_2F	26.7 (−18.2)	
CH_2–CHF_2	26.7 (−14.5)	
CH_2–CF_3	9.9 (−30.9)	1[b,e]
CHF–CH_3	−17.0 (−52.3)	
CHF–CH_2F	−21.1 (−54.6)	
CHF–CHF_2	−23.4 (−56.1)	
CHF–CF_3	−33.9 (−65.7)	
CF_2–CH_3	−40.1 (−65.3)	96000[b,f]
CF_2–CH_2F	−36.3 (−61.2)	
CF_2–CHF_2	−42.9 (−66.3)	
CF_2–CF_3	−49.7 (−72.6)	1160[b,g]

[a]Values in parentheses are corrected with zero point energy.
[b]Ref. 1.
[c]Ref. 14.
[d]Ref. 17.
[e]Ref. 16.
[f]Ref. 15.
[g]Ref. 6.

When the methyl group or methylene bridge adjacent to the OCO part is not fluorinated, the ΔE value without ZPE correction is calculated to be positive (see Table 1.4), which suggests endothermic decomposition. However, the inclusion of ZPE correction results in negative values of ΔE even for these peroxides. Therefore, one can conclude that the thermal decomposition reaction is exothermic for all peroxides studied in the present work.

In the case of the methyl/fluoromethyl groups, $\Delta E = 20.3$, −25.9, −56.4 and −48.7 kJ mol^{-1} without ZPE correction (−30.7, −66.5, −86.6 and −71.9 kJ mol^{-1} with ZPE correction) for R = CH_3, CH_2F, CHF_2 and CF_3, respectively (see Table 1.4). As mentioned above, fluorination of the methyl group tends to decrease the heat of decomposition. One exception is that ΔE is higher for R = CF_3 than for R = CHF_2, because of the higher BDE of the C–C bond in the latter. In the case of ethyl/fluoroethyl groups, the heat of decomposition is substantially lowered by fluorination of the methylene bridge. The ΔE value without ZPE correction (with ZPE correction) is from 9.9 to 26.7 kJ mol^{-1} (from −30.9 to −14.5 kJ mol^{-1}) for the CH_2 bridge, from −33.9 to −17.0 kJ mol^{-1} (from −65.7 to −52.3 kJ mol^{-1}) for the CHF bridge and from −49.7 to −36.3 kJ mol^{-1} (from −72.6 to −61.2 kJ mol^{-1}) for the CF_2 bridge. Although the difference within each methylene/fluoromethylene bridge is relatively small, ΔE is likely to exhibit the lowest value when the terminal methyl group is perfluorinated, that is, when R = CH_2–CF_3, CHF–CF_3 and CF_2–CF_3 for the methylene bridge CH_2, CHF and CF_2, respectively.

Table 1.4 also gives the rate of decomposition, k_d, for some RC(O)O–OC(O)R peroxides whose decomposition rates have been determined experimentally and reported in the literature.[1,6,14–17] Comparing perfluorinated and non-fluorinated peroxides within each carbon number of the R group, k_d exhibits a good correlation with the heat of decomposition ΔE. The decomposition rate for $R = CF_3$ is much larger than for $R = CH_3$ and the decomposition rate for $R = CF_2–CF_3$ is much larger than for $R = CH_2–CH_3$, as expected from the difference in heat of decomposition. For partially fluorinated peroxides, on the other hand, the correlation between k_d and ΔE seems less clear. In particular, although the decomposition rate of peroxide with $R = CF_2–CH_3$ is extremely large compared with those of other peroxides summarized in Table 1.4, the corresponding heat of decomposition is considerably higher than that of perfluorinated peroxides ($R = CF_3$ and $CF_2–CF_3$). This result suggests that heat of reaction is not the only factor that determines the reactivity of thermal decomposition. It would be necessary to consider the whole energy profile for the decomposition to elucidate further the effects of fluorination on the decomposition rate.

Figure 1.5 shows a schematic representation of the energy profile expected for the thermal decomposition of RC(O)O–OC(O)R peroxides. In the present work, we optimized the lowest-energy structures of RC(O)O–OC(O)R, RC(O)O$^\bullet$, R$^\bullet$ and CO_2 and calculated the electronic energies of these compounds at the optimized geometry. BDE and heat of decomposition were calculated as the energy differences among these lowest-energy structures. The existence of energy minima for RC(O)O$^\bullet$ and R$^\bullet$ radicals suggests that there could exist a reaction path for the thermal decomposition in the stepwise mechanism consisting of reactions of eqn (1.1) and (1.2), as shown in Figure 1.5. This reaction path also suggests that a transition state should

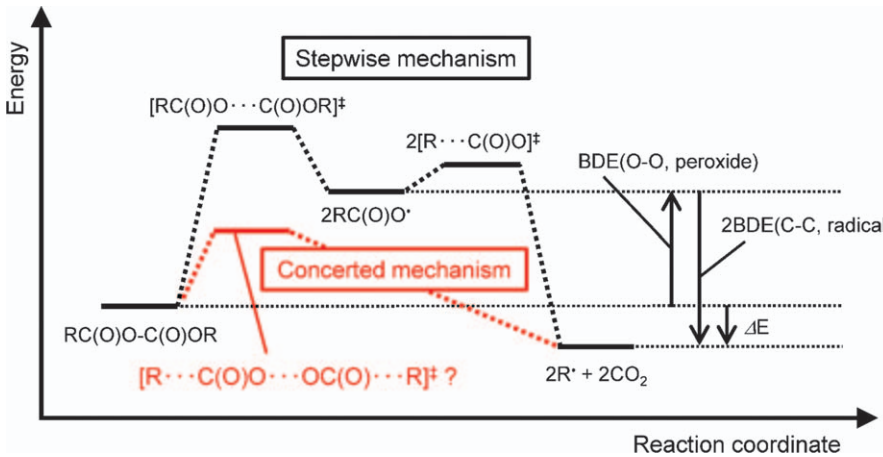

Figure 1.5 Schematic representation of the energy profile for the thermal decomposition of RC(O)O–OC(O)R peroxide *via* stepwise and concerted mechanisms.

be found for each step of the decomposition. In Figure 1.5, these transition-state structures are labeled $[RC(O)O\cdots OC(O)R]^{\ddagger}$ and $[R\cdots C(O)O]^{\ddagger}$. For $R = CH_3$ and CF_3, Gu *et al.*[8] located transition-state structures corresponding to $[RC(O)O\cdots OC(O)R]^{\ddagger}$ and $[R\cdots C(O)O]^{\ddagger}$.

For the full understanding of the mechanism and kinetics of thermal decomposition, it would be necessary to find transition-state structure for the single-step decomposition reaction of eqn (1.3), labeled $[R\cdots C(O)O\cdots OC(O)\cdots R]^{\ddagger}$ in Figure 1.5. Locating (or trying to locate) this type of transition state is important for two reasons. First, if the transition state $[R\cdots C(O)O\cdots OC(O)\cdots R]^{\ddagger}$ exists, the activation energy calculated from the energy difference between this transition-state structure and the RC(O)O–OC(O)R minimum structure determines the rate of decomposition in the concerted mechanism. Second, by comparing the energy of transition states $[R\cdots C(O)O\cdots OC(O)\cdots R]^{\ddagger}$ and $[R\cdots C(O)O]^{\ddagger}$ (the latter energy should be multiplied by two), one can determine whether the decomposition of RC(O)O–OC(O)R peroxide proceeds according to the concerted or stepwise mechanism.

Interestingly, fluorination of the R group is expected to stabilize the transition state $[R\cdots C(O)O\cdots OC(O)\cdots R]^{\ddagger}$ significantly, because this fluorination largely reduces the C–C BDE (see Table 1.3). This expected energy change suggests that the concerted mechanism might become more preferred in fluoroalkanoyl peroxides and thus would be consistent with the scenario that non-fluorinated and fluorinated alkanoyl peroxides exhibit stepwise and concerted decomposition mechanisms, respectively. Hence examination of the $[R\cdots C(O)O\cdots OC(O)\cdots R]^{\ddagger}$ transition state is critical to elucidate the mechanism of decomposition. This calculation would be a challenging task, because the molecular system around this transition state may be regarded as a radical with four unpaired electrons and then the electronic structure calculation of this system needs a multi-reference molecular orbital method.

1.4 Conclusion

In this chapter, we have examined molecular structures, bond strengths and heats of decomposition of alkanoyl/fluoroalkanoyl peroxides by means of *ab initio* electronic structure calculations. The present computational results strongly suggest that the C–C bond is significantly weakened by fluorination of the alkyl group. The O–O bond, on the other hand, is less likely to be affected by fluorination. In particular, the present results show that fluorination on the C atom adjacent to the OCO part reduces the C–C bond dissociation energy considerably, supporting previous computational results of semiempirical calculations.[6] Hence the strength of the C–C bond is expected to play an essential role in determining the reaction mechanism and kinetics of thermal decomposition in alkanoyl and fluoroalkanoyl peroxides. In future work, it would be important to calculate the whole energy profile for thermal decomposition in the concerted mechanism and that in the

stepwise mechanism, especially transition states for these reactions, and to confirm which mechanism is more preferred in each peroxide.

Acknowledgements

The authors thank Yutaro Honda and Akira Sawada for substantial contributions to the present work. S.Y. acknowledges financial support from a Hirosaki University Grant for Exploratory Research by Young Scientists and Newly-Appointed Scientists.

References

1. H. Sawada, *Chem. Rev.*, 1996, **96**, 1779.
2. O. H. Bullitt, *US Pat.*, 2559630, 1951.
3. D. M. Young and W. N. Stoops, *US Pat.*, 2792423, 1957.
4. M. Yoshida, H. Amemiya, M. Kobayashi, H. Sawada, H. Hagii and K. Aoshima, *J. Chem. Soc., Chem. Commun.*, 1985, 234.
5. H. Sawada, M. Yoshida, H. Hagii, K. Aoshima and M. Kobayashi, *Bull. Chem. Soc. Jpn.*, 1986, **59**, 215.
6. H. Sawada, M. Nakayama, O. Kikuchi and Y. Yokoyama, *J. Fluorine Chem.*, 1990, **50**, 393.
7. R. D. Bach, P. Y. Ayala and H. B. Schlegel, *J. Am. Chem. Soc.*, 1996, **118**, 12758.
8. Z. H. Gu, Y. X. Wang and P. B. Balbuena, *J. Phys. Chem. A*, 2006, **110**, 2448.
9. Y. Z. Zhou, S. Li, Q. S. Li and S. W. Zhang, *J. Mol. Struct.: THEOCHEM*, 2008, **854**, 40.
10. T. Noro, M. Sekiya and T. Koga, *Theor. Chem. Acc.*, 2012, **131**, 1124.
11. M. W. Schmidt, K. K. Baldridge, J. A. Boatz, S. T. Elbert, M. S. Gordon, J. H. Jensen, S. Koseki, N. Matsunaga, K. A. Nguyen, S. Su, T. L. Windus, M. Dupuis and J. A. Montgomery Jr., *J. Comput. Chem.*, 1993, **14**, 1347.
12. R. Kopitzky, H. Willner, A. Hermann and H. Oberhammer, *Inorg. Chem.*, 2001, **40**, 2693.
13. H. Oberhammer, *ChemPhysChem*, 2015, **16**, 282.
14. *Polymer Handbook*, ed. J. Brandrup and E. H. Irmnergut, Wiley-Interscience, New York, 2nd edn, 1975.
15. M. V. Zhuravlev, A. I. Burmakov, F. A. Bloshchitsa, V. P. Sass and S. V. Sokolov, *Zh. Org. Khim.*, 1982, **18**, 1825.
16. M. V. Zhuravlev, V. P. Sass and S. V. Sokolov, *Zh. Org. Khim.*, 1983, **19**, 44.
17. H. Sawada, M. Nakayama, M. Yoshida, T. Yoshida and N. Kamigata, *J. Fluorine Chem.*, 1990, **46**, 423.